Physics of Fluids

RESEARCH ARTICLE | JULY 12 2023

Nonlinear ultrasound propagation in liquid containing multiple microbubbles coated by shell incorporating anisotropy

Kawahata Ryoki (川畠稜輝) ; Kanagawa Tetsuya (金川哲也) ; Georges Chabouh

Physics of Fluids 35, 073312 (2023)
https://doi.org/10.1063/5.0141983

Physics of Fluids ARTICLE scitation.org/journal/phf

Nonlinear ultrasound propagation in liquid containing multiple microbubbles coated by shell incorporating anisotropy

Cite as: Phys. Fluids **35**, 073312 (2023); doi: 10.1063/5.0141983
Submitted: 10 January 2023 · Accepted: 17 March 2023 ·
Published Online: 12 July 2023

Ryoki Kawahata (川畠稜輝),[1] Tetsuya Kanagawa (金川哲也),[2,a)] and Georges Chabouh[3]

AFFILIATIONS

[1]Department of Engineering Mechanics and Energy, Graduate School of Systems and Information Engineering, University of Tsukuba, Tsukuba 305-8573, Japan
[2]Department of Engineering Mechanics and Energy, Institute of Systems and Information Engineering, University of Tsukuba, Tsukuba 305-8573, Japan
[3]Sorbonne Université, UMR 7371 CNRS, Inserm U1146, Laboratoire d'Imagerie Biomédicale, 15 Rue de l'Ecole de Médecine, 75006 Paris, France

[a)]Author to whom correspondence should be addressed: kanagawa.tetsuya.fu@u.tsukuba.ac.jp

ABSTRACT

Using microbubbles coated by a thin shell as ultrasound contrast agents for ultrasound diagnosis improves image resolution. Since numerous microbubbles are used in clinical practice, understanding the acoustic properties of liquids containing multiple microbubbles is important. However, interactions between ultrasound and numerous coated microbubbles have not been fully investigated theoretically. Additionally, ultrasound contrast agents with shells made of various materials have been developed. Recently, an equation of motion that considers the anisotropy of the shell was proposed [Chabouh *et al.*, "Spherical oscillations of encapsulated microbubbles: Effect of shell compressibility and anisotropy," J. Acoust. Soc. Am. **149**, 1240 (2021)], and the effect of shell anisotropy on the resonance of the oscillating bubble was reported. In this study, we derived a nonlinear wave equation describing ultrasound propagation in liquids containing numerous coated microbubbles based on the method of multiple scales by expanding Chabouh's equation of motion for the single bubble. This was achieved by considering shell anisotropy in the volumetric average equation for the liquid and gas phases. Shell anisotropy was observed to affect the advection, nonlinearity, attenuation, and dispersion of ultrasound. In particular, the attenuation effects increased or decreased depending on the anisotropic shell elasticity.

I. INTRODUCTION

The resolution of ultrasound images improves considerably when microbubbles are used as contrast agents during diagnosis.[1–3] In general, contrast bubbles are covered with a thin membrane (or shell) of lipids[4–7] and other substances.[8–10] A deep understanding of microbubble/ultrasound interaction from a physical perspective is the key to solve issues in ultrasound contrast imaging and diagnosis. From a mathematical perspective, many equations of motion for a coated bubble have been proposed by considering a single bubble.[11–26] The first mathematical model for an ultrasound contrast agent (UCA) was developed by de Jong *et al.*[11] based on *ad hoc* physical properties. Church[12] developed a theoretical model by modeling the shell of a coated bubble similar to a Kelvin–Voigt model under the assumption that the shell is viscoelastic. Hoff *et al.*[13] reformulated the equations of motion such that outer particle radius was the only variable. Church[12] and Hoff *et al.*[13] proposed mathematical models from a mechanical perspective, considering the shell to be a viscoelastic body (i.e., continuum), and established the pioneering theory of the nonlinear oscillations of a UCA.

Ultrasound attenuation is important for diagnosis; specifically, three maximum possible suppression of ultrasound attenuation is desired. On the other hand, non-linearity of coated microbubbles generates higher harmonic components, and it helps to shut down the tissue signal and then contributes to the improvement of image resolution.[27] In a clinical practice, indeed, numerous coated microbubbles are injected. Therefore, clarifying the propagation properties of ultrasound in a liquid with numerous contrast bubbles is necessary. Previous models[11–23] were limited to a single contrast agent. However,

various studies[28–30] investigated the bubble–bubble interactions. Colonius group[31] showed the importance of incorporating the shift in resonance in the linear regime with experimental evidence. Recent progress by Sojahrood group studied the pressure dependence effects and nonlinear large amplitude bubble oscillations[32–37] in the case of bubbly media. Experiments have been performed to investigate the attenuation and speed of ultrasound.[11,13–15,21,29,33,38–47] Another recent progress should be also mentioned.[48–61] There are also studies that use the Helmholtz model for pressure.[32,62,63] However, further investigations in the case of multiple contrast agents are still lacking. In addition, our group recently extended Church's mathematical model[12] for a single contrast agent to multiple contrast agents[64] and extended Chabouh's model[65] considering the shell compressibility of a single bubble to multiple microbubbles.[66,67]

Generally, shells comprise various materials, such as lipids,[4–7] polymers,[8] and proteins,[9,10] distributed in naturally occurring anisotropic layers that contribute to the acoustic properties of bubbles and ultrasound propagation. Recently, Chabouh *et al.*[68] reported that shell anisotropy can explain the experimental buckled shape of UCAs. They introduced a characteristic distance for elasticity d_{eff} that is equal to the thickness d for a thin shell of an isotropic material. However, all previous models (e.g., Refs. 11–19, 29, and 69) assumed the shell to be an isotropic material. Recently, an updated equation of motion describing the oscillation of a single bubble with an anisotropic shell was proposed by Chabouh, and the contribution of shell anisotropy to oscillations was reported.[65] The purpose of this study is to extend that model for a single contrast agent with shell anisotropy[65] to multiple contrast agents and construct a mathematical model.

The remainder of this paper is organized as follows: Sec. II introduces the formulation of our model and assumptions, Sec. III presents the derivation of the Korteweg–de Vries–Burgers (KdVB) equation describing ultrasound propagation and the investigation of the effects of shell anisotropy, Sec. IV presents the limitations of our model and future perspective, and Sec. V presents the summary of our study.

II. FORMULATION OF THE PROBLEM

A. Problem statement

The focus of this study is the weak nonlinear propagation (i.e., finite but small amplitude) of one-dimensional and progressive pressure waves radiating from a source in liquids containing coated microbubbles. Although the viscoelastic shell is assumed to correspond to a Kelvin–Voigt model in many previous studies, we assumed a purely elastic shell (i.e., without considering the viscosity of the shell) according to Chabouh's model[65] as a first step in previous studies. In this study, the anisotropy of the shell[65] has been newly incorporated. As shown in Fig. 1, the material properties are assumed to differ radially and orthoradially, i.e., we consider a transversely anisotropic material, which is a special case of general anisotropy. Only low frequencies and long wavelengths are focused on in this paper. For simplicity, the following assumptions are made:

(i) Shell anisotropy is newly considered. The thickness of the shell is considered to be a constant d_0^*.
(ii) The shell of the bubble is considered to be a purely elastic body.
(iii) Initially, the liquid is at rest, and the bubbles are uniformly distributed.
(iv) The oscillations of bubbles are spherically symmetric.
(v) The bubbles are filled with a non-condensable ideal gas.
(vi) Liquid compressibility is considered.
(vii) The bubbles do not coalesce, break up, appear, or disappear.
(viii) Thermal conduction[67,70–73] and phase change[74–76] are disregarded since they are not expected to have a significant impact on ultrasound diagnosis.
(ix) Bubble–bubble interactions[20,30,31,77,78] are not considered.
(x) Drag force[67,79,80] acting on the bubbles is ignored.

Bubble–bubble interactions[28–32] are an important effect, but they were not considered in our study for simplicity. Wave propagation in

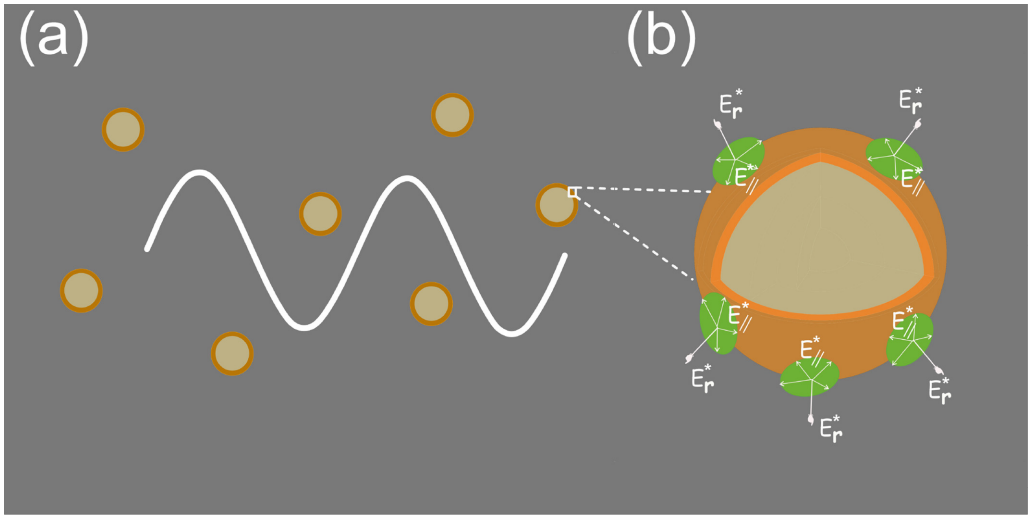

FIG. 1. (a) Sketch of the ultrasound propagation in liquids containing multiple coated bubbles, zoom on the shell of the microbubble made from anisotropic material. (b) Transverse anisotropic case is considered where the radial Young modulus E_r^* is different from the in-plane Young modulus $E_{||}^*$. In the case of isotropic material, the value of E_r^* is equal to $E_{||}^*$.[65]

bubbly media considering bubble–bubble interactions has been investigated in the linear regime by Commander and Prosperetti[28] and Fuster *et al.*[31] Further, Sojahrood *et al.* investigated the effects of attenuation and sound speed of the wave on bubble–bubble interactions in both the linear and nonlinear regimes.[29,30,32]

B. Basic equations

The equation of motion for a bubble coated with an anisotropic shell[65] was used,

$$\rho^*_{\mathrm{L}0}\left(1-\frac{1}{c^*_{\mathrm{L}0}}\frac{\mathrm{D_G}R^*}{\mathrm{D}t^*}\right)R^*\frac{\mathrm{D^2_G}R^*}{\mathrm{D}t^{*2}}+\frac{3}{2}\rho^*_{\mathrm{L}0}\left(1-\frac{1}{3c^*_{\mathrm{L}0}}\frac{\mathrm{D_G}R^*}{\mathrm{D}t^*}\right)\left(\frac{\mathrm{D_G}R^*}{\mathrm{D}t^*}\right)^2 = \left(1+\frac{1}{c^*_{\mathrm{L}0}}\frac{\mathrm{D_G}R^*}{\mathrm{D}t^*}\right)P^*+\frac{R^*_0}{c^*_{\mathrm{L}0}}\frac{\mathrm{D_G}}{\mathrm{D}t^*}\left(p^*_{\mathrm{L}}+P^*\right), \tag{1}$$

and the balance of normal stress across the bubble–liquid interface is as follows:

$$P^* = -4\mu^*_{\mathrm{L}}\frac{1}{R^*}\frac{\mathrm{D_G}R^*}{\mathrm{D}t^*}-p^*_{\mathrm{L}}-\frac{2\sigma^*_2}{R^*}+p^*_{\mathrm{G}}-\frac{2\sigma^*_1}{R^*-d^*_0} - U^{*2}\rho^*_{\mathrm{L}0}K_{\mathrm{ani}}\left(1-\frac{R^*_0}{R^*}\right), \tag{2}$$

where the superscript * denotes a dimensional quantity; t is the time, p is the volumetric averaged pressure, P is the surface averaged liquid pressure at an interface $c_{\mathrm{L}0}$ is the speed of sound in a pure liquid, R is the bubble radius, ρ is the density, d_0 is the constant shell thickness, μ_{L} is the liquid viscosity, U is the typical propagation speed of a wave, and σ_1 and σ_2 are the surface tensions at the internal and external boundaries of the shell, respectively; the subscripts G and L denote the gas and liquid phases, respectively, and the subscript 0 denotes the bubbles at rest in the initial uniform state. Here, the anisotropic elastic constant K_{ani} is a constant that is determined from the elastic constants of the shell (e.g., $E^*_{||}$, E^*_r, $\nu_{||}$, and $\nu_{\theta r}$), where in Fig. 1, E^*_r is Young's modulus in the radial direction, $\nu_{\theta r}$ is Poisson's ratio with the radial load, and $E^*_{||}$ and $\nu_{||}$ are Young's modulus and Poisson's ratio in the orthoradial plane, respectively.[65] Since the explicit form of the constant K_{ani} is complex, it is presented in Appendix A.

Further, the following mass and momentum conservation equations for a bubbly liquid based on two-fluid model[64,66,81,82] were used:

(i) Mass conservation equation for the gas phase:

$$\frac{\partial}{\partial t^*}\left(\alpha\rho^*_{\mathrm{G}}\right)+\frac{\partial}{\partial x^*}\left(\alpha\rho^*_{\mathrm{G}}u^*_{\mathrm{G}}\right)=0. \tag{3}$$

(ii) Mass conservation equation for the liquid phase:

$$\frac{\partial}{\partial t^*}\left[(1-\alpha)\rho^*_{\mathrm{L}}\right]+\frac{\partial}{\partial x^*}\left[(1-\alpha)\rho^*_{\mathrm{L}}u^*_{\mathrm{L}}\right]=0. \tag{4}$$

(iii) Momentum conservation equation for the gas phase:

$$\frac{\partial}{\partial t^*}\left(\alpha\rho^*_{\mathrm{G}}u^*_{\mathrm{G}}\right)+\frac{\partial}{\partial x^*}\left(\alpha\rho^*_{\mathrm{G}}u^{*2}_{\mathrm{G}}\right)+\alpha\frac{\partial p^*_{\mathrm{G}}}{\partial x^*}=F^*. \tag{5}$$

(iv) Momentum conservation equation for the liquid phase:

$$\frac{\partial}{\partial t^*}\left[(1-\alpha)\rho^*_{\mathrm{L}}u^*_{\mathrm{L}}\right]+\frac{\partial}{\partial x^*}\left[(1-\alpha)\rho^*_{\mathrm{L}}u^{*2}_{\mathrm{L}}\right] + (1-\alpha)\frac{\partial p^*_{\mathrm{L}}}{\partial x^*}+P^*\frac{\partial\alpha}{\partial x^*}=-F^*. \tag{6}$$

Here, x is the space coordinate and α is the void fraction (i.e., volume fraction of gas phase). Further, an interfacial momentum transport F^* was introduced according to the virtual mass force model as follows:[82,84]

$$F^* = -\beta_1\alpha\rho^*_{\mathrm{L}}\left(\frac{\mathrm{D_G}u^*_{\mathrm{G}}}{\mathrm{D}t^*}-\frac{\mathrm{D_L}u^*_{\mathrm{L}}}{\mathrm{D}t^*}\right) - \beta_2\rho^*_{\mathrm{L}}\left(u^*_{\mathrm{G}}-u^*_{\mathrm{L}}\right)\frac{\mathrm{D_G}\alpha}{\mathrm{D}t^*}-\beta_3\alpha\left(u^*_{\mathrm{G}}-u^*_{\mathrm{L}}\right)\frac{\mathrm{D_G}\rho^*_{\mathrm{L}}}{\mathrm{D}t^*}, \tag{7}$$

where the constants β_1, β_2, and β_3 can be set to 1/2 for spherical bubbles, and the definitions of the operators $\mathrm{D_G}/\mathrm{D}t^*$ and $\mathrm{D_L}/\mathrm{D}t^*$ are defined as

$$\frac{\mathrm{D_G}}{\mathrm{D}t^*}\equiv\frac{\partial}{\partial t^*}+u^*_{\mathrm{G}}\frac{\partial}{\partial x^*},\quad \frac{\mathrm{D_L}}{\mathrm{D}t^*}\equiv\frac{\partial}{\partial t^*}+u^*_{\mathrm{L}}\frac{\partial}{\partial x^*}. \tag{8}$$

(v) Tait equation of state for a liquid is

$$p^*_{\mathrm{L}}=p^*_{\mathrm{L}0}+\frac{\rho^*_{\mathrm{L}0}c^{*\,2}_{\mathrm{L}0}}{n}\left[\left(\frac{\rho^*_{\mathrm{L}}}{\rho^*_{\mathrm{L}0}}\right)^n-1\right], \tag{9}$$

where n is the material constant (e.g., $n=7.15$ for water).

(vi) Polytropic equation of state for gases is

$$\frac{p^*_{\mathrm{G}}}{p^*_{\mathrm{G}0}}=\left(\frac{\rho^*_{\mathrm{G}}}{\rho^*_{\mathrm{G}0}}\right)^\gamma, \tag{10}$$

where γ is the polytropic exponent.

(vii) Conservation equation for the mass inside a bubble is

$$\left(\frac{\rho^*_{\mathrm{G}}}{\rho^*_{\mathrm{G}0}}\right)=\left(\frac{R^*_0}{R^*}\right)^3. \tag{11}$$

C. Nondimensionalization

For nondimensional time $t=t^*/T^*$ and space coordinate $x=x^*/L^*$ (T^* and L^* are typical period and wavelength, respectively), using the nondimensionalized independent variables t and x, near-field [i.e., the temporal and spatial scales of $\mathcal{O}(1)$] is defined by

$$t_0=t,\quad x_0=x, \tag{12}$$

and far-field [i.e., the temporal and spatial scales of $\mathcal{O}(1/\epsilon)$] is by

$$t_1=\epsilon t,\quad x_1=\epsilon x, \tag{13}$$

where $\epsilon\,(\ll 1)$ is the nondimensional wave amplitude. The differential operators are then introduced based on the derivative expansion method,[83]

$$\frac{\partial}{\partial t}=\frac{\partial}{\partial t_0}+\epsilon\frac{\partial}{\partial t_1},\quad \frac{\partial}{\partial x}=\frac{\partial}{\partial x_0}+\epsilon\frac{\partial}{\partial x_1}. \tag{14}$$

Next, all the dependent variables are nondimensionalized and expanded in a power series of ϵ, as follows:

$$\frac{\alpha}{\alpha_0}=1+\epsilon\alpha_1+\epsilon^2\alpha_2+\cdots, \tag{15}$$

$$\frac{u_{\mathrm{G}}^*}{U^*}=\epsilon u_{\mathrm{G1}}+\epsilon^2 u_{\mathrm{G2}}+\cdots, \tag{16}$$

$$\frac{u_{\mathrm{L}}^*}{U^*}=\epsilon u_{\mathrm{L1}}+\epsilon^2 u_{\mathrm{L2}}+\cdots, \tag{17}$$

$$\frac{R^*}{R_0^*}=1+\epsilon R_1+\epsilon^2 R_2+\cdots, \tag{18}$$

$$\frac{\rho_{\mathrm{L}}^*}{\rho_{\mathrm{L0}}^*}=1+\epsilon^2\rho_{\mathrm{L1}}+\cdots, \tag{19}$$

$$\frac{p_{\mathrm{L}}^*}{\rho_{\mathrm{L0}}^* U^{*2}}=p_{\mathrm{L0}}+\epsilon p_{\mathrm{L1}}+\epsilon^2 p_{\mathrm{L2}}+\cdots. \tag{20}$$

Since this study focuses on low-frequency long waves, we impose the following relations:[64,66,82,84]

$$\frac{U^*}{c_{\mathrm{L0}}^*}\equiv\mathcal{O}(\sqrt{\epsilon})\equiv V\sqrt{\epsilon},\quad \frac{\omega^*}{\omega_{\mathrm{B}}^*}\equiv\mathcal{O}(\sqrt{\epsilon})\equiv\Omega\sqrt{\epsilon},\quad \frac{R_0^*}{L^*}\equiv\mathcal{O}(\sqrt{\epsilon})\equiv\Delta\sqrt{\epsilon}, \tag{21}$$

where V, Δ, and Ω are constants of $\mathcal{O}(1)$, c_{L0}^* is the speed of sound in a pure liquid, ω^* is the typical angular frequency of the waves, and ω_{B}^* is the eigenfrequency of linear spherical symmetric oscillations in a single bubble. In addition, all dimensional constants (e.g., E_r^*) are nondimensionalized and their orders are estimated as follows:

$$\frac{E_r^*}{\rho_{\mathrm{L0}}^* U^{*2}}\equiv\mathcal{O}(1)\equiv E_r,\quad \frac{E_{\|}^*}{\rho_{\mathrm{L0}}^* U^{*2}}\equiv\mathcal{O}(1)\equiv E_{\|}, \tag{22}$$

$$\frac{\sigma_1^*}{\rho_{\mathrm{L0}}^* U^{*2}(R_0^*-d_0^*)}=\sigma_1,\quad \frac{\sigma_2^*}{\rho_{\mathrm{L0}}^* U^{*2} R_0^*}=\sigma_2,\quad \frac{d_0^*}{R_0^*}=\epsilon d_0, \tag{23}$$

$$\frac{\mu_{\mathrm{L}}^*}{\rho_{\mathrm{L0}}^* U^{*2} T^*}=\epsilon\mu_{\mathrm{L}}. \tag{24}$$

III. RESULTS

A. Linear approximation

Combining the leading-order approximation results of the basic equations, we can derive a single linear wave equation.

(i) Mass conservation equation for the gas phase:

$$\frac{\partial\alpha_1}{\partial t_0}-3\frac{\partial R_1}{\partial t_0}+\frac{\partial u_{\mathrm{G1}}}{\partial x_0}=0. \tag{25}$$

(ii) Mass conservation equation for the liquid phase:

$$\alpha_0\frac{\partial\alpha_1}{\partial t_0}-(1-\alpha_0)\frac{\partial u_{\mathrm{L1}}}{\partial x_0}=0. \tag{26}$$

(iii) Momentum conservation equation for the gas phase:

$$\beta_1\frac{\partial u_{\mathrm{G1}}}{\partial t_0}-\beta_1\frac{\partial u_{\mathrm{L1}}}{\partial t_0}-3\gamma p_{\mathrm{G0}}\frac{\partial R_1}{\partial x_0}=0. \tag{27}$$

(iv) Momentum conservation equation for the liquid phase:

$$(1-\alpha_0+\beta_1\alpha_0)\frac{\partial u_{\mathrm{L1}}}{\partial t_0}-\beta_1\alpha_0\frac{\partial u_{\mathrm{G1}}}{\partial t_0}+(1-\alpha_0)\frac{\partial p_{\mathrm{L1}}}{\partial x_0}=0. \tag{28}$$

(v) Equation of motion as bubble dynamics:

$$R_1+\frac{\Omega^2}{\Delta^2}p_{\mathrm{L1}}=-\sigma_1 d_0. \tag{29}$$

We obtain the linear wave equation for the first-order perturbation of bubble radius R_1 by eliminating α_1, u_{G1}, u_{L1}, and p_{L1} from (25)–(29):

$$\frac{\partial^2 R_1}{\partial t_0^2}-v_{\mathrm{p}}\frac{\partial^2 R_1}{\partial x_0^2}=0, \tag{30}$$

with the phase velocity v_{p},

$$v_{\mathrm{p}}=\sqrt{\frac{3\alpha_0(1-\alpha_0+\beta_1)\gamma p_{\mathrm{G0}}+\beta_1(1-\alpha_0)\Delta^2/\Omega^2}{3\beta_1\alpha_0(1-\alpha_0)}}. \tag{31}$$

Note that v_{p} is the phase velocity containing K_{ani}, i.e., the anisotropy of the shell contributes to the phase velocity. Transforming in v_{p}, we obtain U^* as follows:

$$U^*=\sqrt{\frac{3\alpha_0(1-\alpha_0+\beta_1)\gamma p_{\mathrm{G0}}^*/\rho_{\mathrm{L0}}^*+\beta_1(1-\alpha_0)R_0^{*2}\omega_{\mathrm{B}}^{*2}}{3\beta_1\alpha_0(1-\alpha_0)}}, \tag{32}$$

where ω_{B}^* is derived from the equation of motion for a single bubble (1):

$$\omega_{\mathrm{B}}^*=\sqrt{-\frac{\sigma_2^*}{R_0^*}-2A_{\mathrm{ani}}\frac{\sigma_1^*}{R_0^*}+3A_{\mathrm{ani}}\gamma p_{\mathrm{G0}}^*+K_{\mathrm{ani}}\rho_{\mathrm{L0}}^* U^{*2}}, \tag{33}$$

where A_{ani} and K_{ani} are constants that describe shell anisotropy and have a complex explicit form (see Appendix A). Figure 2 shows the dependence of U^* on α_0. We used the linear approximation resonance frequency ω_{B}^* for a single bubble for simplicity. Remarking that studies on resonance frequency considering bubble–bubble interactions by Yasui *et al.*[77] and Guédra *et al.*[85] are also significant to further extension. We shall include this effect in a future study.

Here, we focus on the right-running wave, set $v_{\mathrm{p}}=1$, and introduce the phase function φ_0:

$$\varphi_0\equiv x_0-t_0. \tag{34}$$

We can express α_1, u_{G1}, u_{L1}, and p_{L1} as a function $R_1(\varphi_0)$ by rewriting (25)–(29) with φ_0 and integrating them with respect to φ_0:

$$\alpha_1=s_1R_1,\quad u_{\mathrm{G1}}=s_2R_1,\quad u_{\mathrm{L1}}=s_3R_1,\quad p_{\mathrm{L1}}=s_4R_1,$$
$$s_4=-\frac{\Delta^2}{\Omega^2},\quad s_1=\frac{(1-\alpha_0)[3\beta_1\alpha_0-(1-\alpha_0)s_4]}{\alpha_0(1-\alpha_0+\beta_1)},\quad s_2=s_1-3,\quad s_3=-\frac{\alpha_0 s_1}{1-\alpha_0}. \tag{35}$$

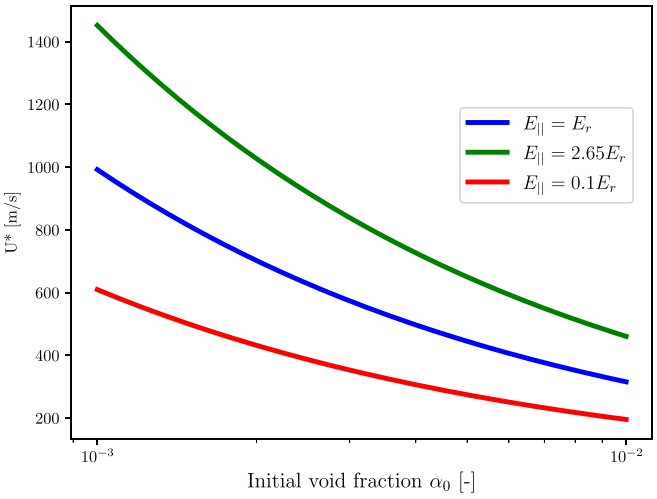

FIG. 2. Wave propagation speed U^* vs initial void fraction α_0: $\Omega = 1$, $\sqrt{\epsilon} = 0.15$, $v_p = 1$, $R_0^* = 1\ \mu$m, $\mu_L^* = 10^{-3}$ Pa s, $\sigma_1^* = 0.005$ N/m, $\sigma_2^* = 0.72$ N/m, $d_0^* = 7.5$ nm, $c_{L0}^* = 1.5 \times 10^3$ m/s, $p_{L0}^* = 101\,325$ Pa, $\gamma = 1.4$, $\rho_{L0}^* = 10^3$ kg/m^3, and $\nu_{\theta r} = \nu_r = 0.35$; (i) anisotropic case 1, i.e., $E_r^* = 88.8$ MPa and $E_{||}^* = 235.32$ MPa, (ii) isotropic case, i.e., $E_r^* = 88.8$ and $E_{||}^* = 88.8$ MPa, and (iii) anisotropic case 2, i.e., $E_r^* = 88.8$ and $E_{||}^* = 8.88$ MPa. These values are also used in Figs. 3 and 4.

B. Nonlinear approximation and resultant KdVB equation

Using the same method as that in Sec. III A, the second-order approximation results of the basic equations are derived as

$$\frac{\partial^2 R_2}{\partial t_0^2} - \frac{\partial^2 R_2}{\partial x_0^2} = \frac{1}{3}\frac{\partial K_1}{\partial \varphi_0} - \frac{1}{3\alpha_0}\frac{\partial K_2}{\partial \varphi_0} + \frac{1-\alpha_0+\beta_1}{3\beta_1(1-\alpha_0)}\frac{\partial K_3}{\partial \varphi_0} + \frac{1}{3\alpha_0(1-\alpha_0)}\frac{\partial K_4}{\partial \varphi_0} - \frac{\Delta^2}{3\alpha_0\Omega^2}\frac{\partial^2 K_5}{\partial \varphi_0^2} \equiv K(R_1; \varphi_0, t_1, x_1). \tag{36}$$

The inhomogeneous terms $K_i\,(i = 1, 2, 3, 4, 5)$ are explicitly provided in Appendix B. The solution condition for the inhomogeneous equation in (37) requires $K = 0$, i.e.,

$$2\frac{\partial}{\partial \varphi_0}\left(\frac{\partial R_1}{\partial t_1} + \frac{\partial R_1}{\partial x_1} + \Pi_0\frac{\partial R_1}{\partial \varphi_0} - \Pi_1 R_1\frac{\partial R_1}{\partial \varphi_0} - \Pi_2\frac{\partial^2 R_1}{\partial \varphi_0^2} + \Pi_3\frac{\partial^3 R_1}{\partial \varphi_0^3}\right) = 0. \tag{37}$$

Finally, based on the variable transformation,

$$\tau \equiv \epsilon t, \quad \xi \equiv x - (1 + \epsilon\Pi_0)t, \tag{38}$$

and the second-order approximation results, we derived the KdVB equation considering the shell anisotropy effects, as follows:

$$\frac{\partial R_1}{\partial \tau} - \Pi_1 R_1\frac{\partial R_1}{\partial \xi} - \Pi_2\frac{\partial^2 R_1}{\partial \xi^2} + \Pi_3\frac{\partial^3 R_1}{\partial \xi^3} = 0, \tag{39}$$

where the constant coefficients $\Pi_i\ (i = 0, 1, 2, 3)$ represent advection, nonlinearity, attenuation, and dispersion, respectively. Because (39) is represented as a linear combination of the nonlinear, attenuation, and dispersion terms, we can perform a quantitative comparison of the magnitude of these coefficients. The difference between isotropic and anisotropic cases is reflected in only each coefficient Π_i,

$$\Pi_0 = -\frac{1}{6\alpha_0}\left[\frac{(1-\alpha_0)V^2\Delta^2}{\Omega^2} - 4A_{\text{ani}}\sigma_1 d_0\right], \tag{40}$$

$$\Pi_2 = \frac{1}{6\alpha_0}\left(\frac{\Delta^3 V}{\Omega^2} + 4\mu_L\right), \tag{41}$$

$$\Pi_3 = \frac{\Delta^2}{6\alpha_0}, \tag{42}$$

$$\Pi_1 = -\frac{1}{6}\left[k_1 - \frac{k_2}{\alpha_0} + \frac{(1-\alpha_0+\beta_1)k_3}{\beta_1(1-\alpha_0)} + \frac{k_4}{\alpha_0(1-\alpha_0)} - \frac{2k_5}{\alpha_0}\right], \tag{43}$$

where the explicit forms of $k_i\ (i = 0, 1, 2, 3)$ are given by

$$\begin{aligned} k_1 &= 6(2-s_1) + 2s_2(3-s_1), \quad k_2 = -2\alpha_0 s_1 s_3, \\ k_5 &= \frac{3}{2}\gamma(3\gamma+1)A_{\text{ani}}p_{G0} - A_{\text{ani}}\sigma_1 - \sigma_2 + K_{\text{ani}}, \\ \hat{k} &= (\beta_1+\beta_2)(s_2-s_3)s_1 - \beta_1(s_2^2 - s_3^2), \\ k_3 &= \hat{k} + 3\gamma p_{G0}(s_1 - 3\gamma - 1), \\ k_4 &= -\alpha_0\hat{k} + \alpha_0 s_1 s_4 - 2(1-\alpha_0)s_3^2 - 2\alpha_0 s_1 s_3. \end{aligned} \tag{44}$$

In Sec. III C, we shall clarify the effect of shell anisotropy in detail by focusing on the functional form of Π_i.

C. Effect of shell anisotropy

Herein, the coefficients of advection (40), nonlinear (43) and (44), attenuation (41), and dispersion (42) in the KdVB equation (39) were investigated quantitatively. All the coefficients were affected by shell anisotropy, and these impacts were positive and negative compared to those in the case with isotropy, respectively.

A graph of each coefficient is presented below. For simplicity, similar to Chabouh *et al.*,[65] we focus on the case where the Poisson ratio is 0.35. We consider the following three cases of $E_{||}^*$ to express shell anisotropy:[65] (i) $E_r^* < E_{||}^*$ as anisotropic case 1, (ii) $E_r^* = E_{||}^*$ as isotropic case, and (iii) $E_r^* > E_{||}^*$ as anisotropic case 2.

In Fig. 2, we plot the wave propagation speed U^* in function of the initial void fraction α_0, for three different above-mentioned cases. Indeed, the wave propagation speed drops with the percentage of bubbles in the medium. On the other hand, the more rigid the medium (anisotripic case 2, i.e., $E_r^* > E_{||}^*$), the faster the wave propagates. Figure 3 shows the advection, nonlinear, attenuation, and dispersion coefficients (i.e., Π_0, Π_1, Π_2, and Π_3) with respect to the initial void fraction α_0. In Fig. 4, each coefficient is investigated for ultrasound diagnosis applications with a lower α_0 than that in Fig. 3. Figure 4 shows the same response for each coefficient to α_0 as Fig. 3. In anisotropy case 1, shell anisotropy suppresses attenuation Π_2 and nonlinearity Π_1. As shown in Fig. 3, Π_1 is not significantly affected by α_0. The differences among the three cases decrease for Π_0 as α_0 increases. Conversely, the differences among the three cases increase for Π_3 as α_0 increases. In ultrasonic diagnosis, the attenuation of ultrasound is an important acoustic characteristic as images are formed using reflected waves. Nonlinearity generates higher harmonics of the wave, improving image resolution. Therefore, suppressing attenuation and

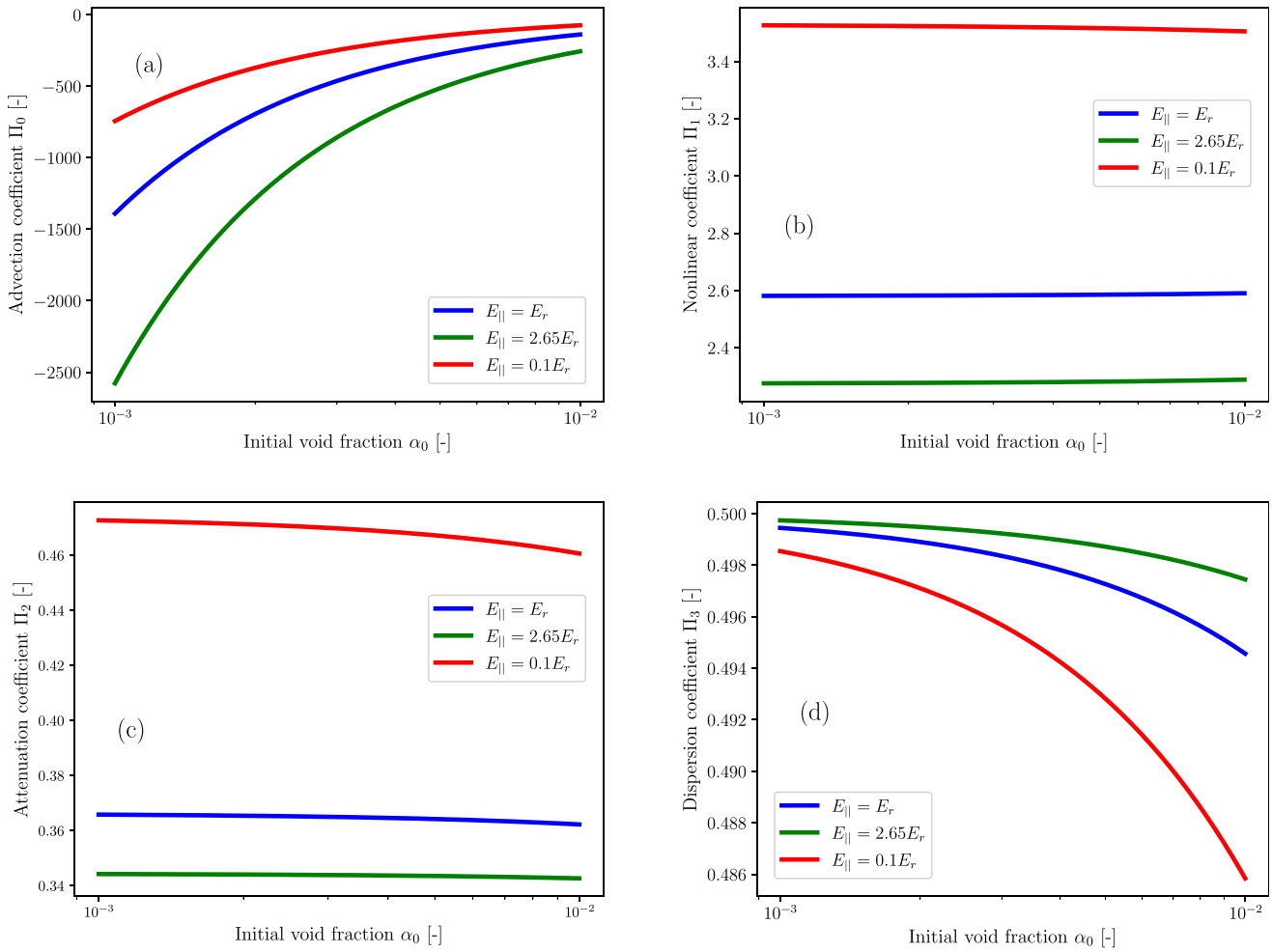

FIG. 3. Coefficients of the KdVB equation vs high initial void fraction α_0: (a) advection Π_0, (b) nonlinearity Π_1, (c) attenuation Π_2, and (d) dispersion Π_3. Here, 2.65 is the upper limit when the Poisson ratio is 0.35 and is calculated by a constraint among elastic constants.[65]

promoting nonlinearity is desirable, i.e., the attenuation coefficient should be anisotropic case 1 and the nonlinear coefficient should be anisotropic case 2.

D. Limitations and future perspective

The use of very short pulses for ultrasound diagnosis applications has been previously reported.[21,86,87] Then, in this study, we focus on the weakly nonlinear (i.e., finite but small amplitude) propagation of ultrasonic waves in liquids containing multiple coated microbubbles. Compared to Hoff's model for a single bubble, the range of applicable nonlinearity is small, i.e., our mathematical model cannot be applied to strong nonlinearity. We obtain (30) from linear approximation and (37) from weakly nonlinear approximation. While pressure should be described in nonlinear regimes for clinical applications, linear and nonlinear pressure models are known to provide different results.[29,62,63]

IV. CONCLUSIONS

To construct a mathematical model for ultrasound diagnosis enhanced by microbubbles, the equation of motion for a single bubble coated with a purely elastic anisotropic shell[65] was extended to the case with multiple bubbles. Shell anisotropy, which entails two different Young's moduli (i.e., E_r^* and $E_{||}^*$), in the radial and orthoradial directions was considered based on Chabouh's model.[65] The KdVB equation for ultrasound propagation in liquids containing multiple coated bubbles was derived using the second-order approximation of basic equations based on the method of multiple scales.

Consequently, shell anisotropy was observed to contribute to the advection, nonlinear, dispersion, and attenuation of ultrasound. In particular, the balance between two Young's moduli (i.e., E_r^* and $E_{||}^*$) can promote and suppress attenuation and nonlinear effects.

In future studies, the current theory and results will be extended to a more general form and applied to real UCA in a biomedical field. The dependence of the Poisson ratio on each coefficient will be

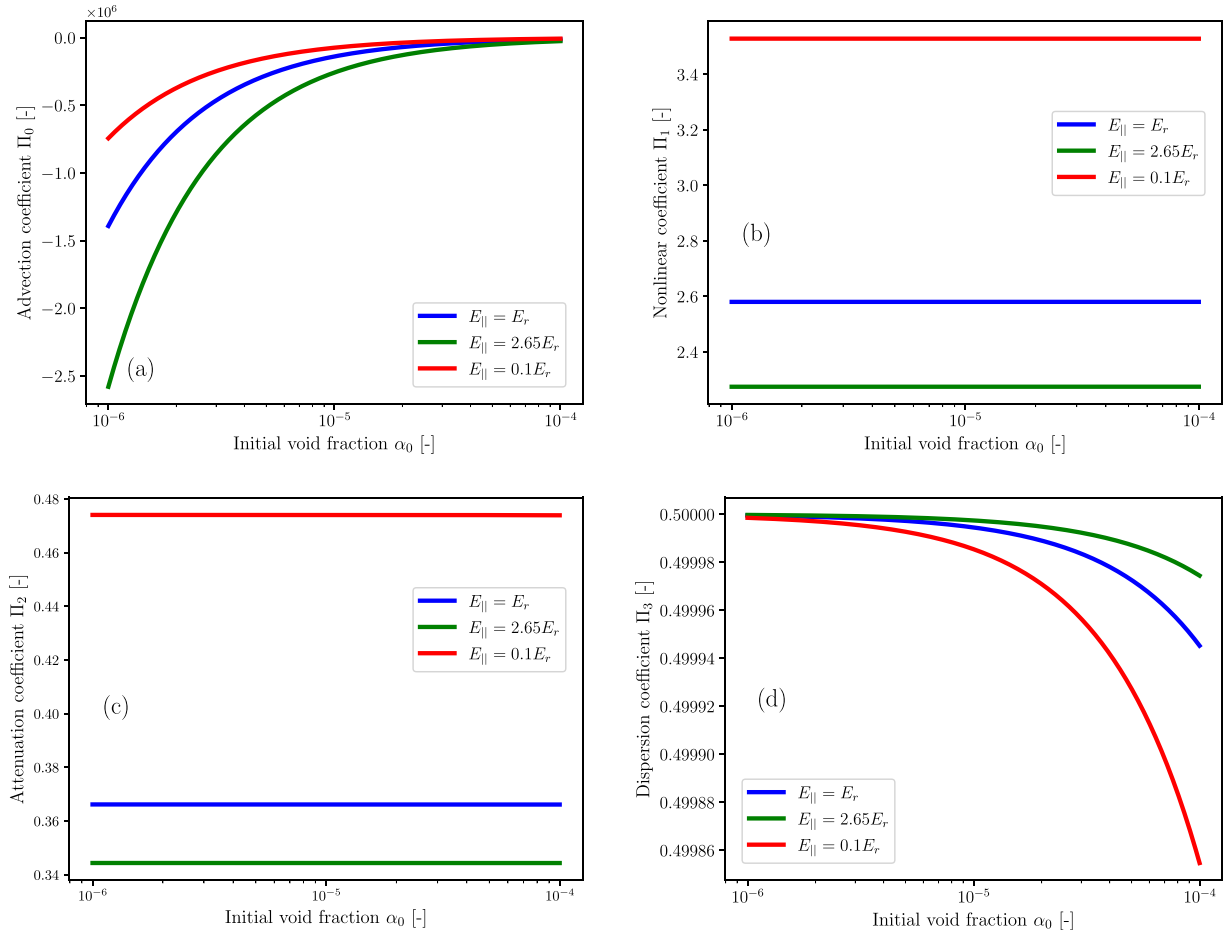

FIG. 4. Coefficients of the KdVB equation vs low initial void fraction α_0: (a) advection Π_0, (b) nonlinearity Π_1, (c) attenuation Π_2, and (d) dispersion Π_3. Here, 2.65 is the upper limit when the Poisson ratio is 0.35 and is calculated by a constraint among elastic constants.[65]

elaborated by constructing a model incorporating a constitutive law describing general shell anisotropy and extending the case of a purely elastic shell to one with a viscoelastic shell.

ACKNOWLEDGMENTS

This work was partially supported by the JSPS KAKENHI (No. 22K03898), based on the results obtained from a project subsidized by the New Energy and Industrial Technology Development Organization (NEDO) (No. JPNP20004) and supported by JKA and its promotion funds from KEIRIN RACE and Ono Charitable Trust for Acoustics. We would like to thank referees for their valuable comments and suggestions and Editage (www.editage.com) for English language editing.

AUTHOR DECLARATIONS

Conflict of Interest

The authors have no conflicts to disclose.

Author Contributions

Ryoki Kawahata: Formal analysis (lead); Investigation (equal); Methodology (equal); Software (lead); Visualization (lead); Writing – original draft (lead); Writing – review & editing (lead). **Tetsuya Kanagawa:** Conceptualization (lead); Formal analysis (supporting); Funding acquisition (lead); Investigation (equal); Methodology (equal); Project administration (lead); Supervision (lead); Writing – original draft (equal); Writing – review & editing (equal). **Georges Chabouh:** Formal analysis (supporting); Investigation (supporting); Methodology (supporting); Writing – original draft (supporting); Writing – review & editing (equal).

DATA AVAILABILITY

The data pertaining to this study are available from the corresponding author upon reasonable request.

APPENDIX A: CONSTANT FOR SHELL OF ANISOTROPY

Elastic constant K_{ani} considering shell anisotropy is given by

$$K_{\mathrm{ani}} = \frac{R_{10}^*(A_{\mathrm{ani}}B_{\mathrm{ani}} + D_{\mathrm{ani}})}{\rho_{\mathrm{L0}}^* U^{*2}\left(1 - \nu_{||} - 2E_{||}^*\nu_{\theta r}^2/E_r^*\right)\left(R_{10}^{*\beta-}R_{20}^{*\beta+} - R_{10}^{*\beta_+}R_{20}^{*\beta-}\right)},$$

where

$$A_{\mathrm{ani}} = \frac{R_{10}^{*\beta_-}R_{20}^{*\beta_+-1}\left[(1-\nu_{||})E_r^*\beta_+ + 2\nu_{\theta r}E_{||}^*\right] - R_{10}^{*\beta_+}R_{20}^{*\beta_--1}\left[(1-\nu_{||})E_r^*\beta_- + 2\nu_{\theta r}E_{||}^*\right]}{R_{10}^{*\beta_+-1}R_{10}^{*\beta_-}\left[(1-\nu_{||})E_r^*\beta_+ + 2\nu_{\theta r}E_{||}^*\right] - R_{10}^{*\beta_--1}R_{10}^{*\beta_+}\left[(1-\nu_{||})E_r^*\beta_- + 2\nu_{\theta r}E_{||}^*\right]}, \tag{A1}$$

$$B_{\mathrm{ani}} = R_{20}^{*\beta_-}R_{10}^{*\beta_+-1}\left[(1-\nu_{||})E_r\beta_+ + 2\nu_{\theta r}E_{||}\right] - R_{20}^{*\beta_+}R_{10}^{*\beta_--1}\left[(1-\nu_{||})E_r\beta_- + 2\nu_{\theta r}E_{||}\right],$$

$$D_{\mathrm{ani}} = R_{20}^{*\beta_+}R_{20}^{*\beta_--1}\left[(1-\nu_{||})E_r\beta_- + 2\nu_{\theta r}E_{||}\right] - R_{20}^{*\beta_-}R_{20}^{*\beta_+-1}\left[(1-\nu_{||})E_r\beta_+ + 2\nu_{\theta r}E_{||}\right], \tag{A2}$$

where T^* is a typical period, E_r^* is the Young modulus in the radial direction, $\nu_{\theta r}$ is the Poisson ratio with radial load, $E_{||}^*$ and $\nu_{||}$ are the Young modulus and the Poisson ratio in the orthoradial direction, respectively,[65] and R_{10}^* and R_{20}^* are the internal and external radius of the shell, respectively. Here, R_{10}^*, R_{20}^*, and shell thickness d_0^* are connected by

$$R_{20}^* = R_{10}^* + d_0^*.$$

Further, $\beta_\pm$ and k are determined as follows:

$$\beta_\pm = \frac{-1 \pm \sqrt{1+8k}}{2}, \quad k = \frac{E_{||}^*(1-\nu_{\theta r})}{E_r^*(1-\nu_{||})}.$$

APPENDIX B: INHOMOGENEOUS TERMS

The explicit form of K_i $(i = 1, 2, 3, 4, 5)$ in (37) is given by

$$K_1 = -\frac{\partial u_{\mathrm{G1}}}{\partial x_1} + \frac{\partial}{\partial t_1}(3R_1 - \alpha_1) + 3\frac{\partial R_1(\alpha_1 - 2R_1)}{\partial t_0} + \frac{\partial}{\partial x_0}[u_{\mathrm{G1}}(3R_1 - \alpha_1)],$$

$$K_2 = (1-\alpha_0)\frac{\partial u_{\mathrm{L1}}}{\partial x_1} - \alpha_0\frac{\partial \alpha_1}{\partial t_1} - \alpha_0\frac{\partial \alpha_1 u_{\mathrm{L1}}}{\partial x_0} + (1-\alpha_0)\frac{\partial \rho_{\mathrm{L1}}}{\partial t_0},$$

$$K_3 = 3\gamma p_{\mathrm{G0}}\frac{\partial R_1}{\partial x_1} - \beta_1\frac{\partial}{\partial t_1}(u_{\mathrm{G1}} - u_{\mathrm{L1}}) - \beta_1\alpha_1\frac{\partial}{\partial t_0}(u_{\mathrm{G1}} - u_{\mathrm{L1}}) - \beta_1\left(u_{\mathrm{G1}}\frac{\partial u_{\mathrm{G1}}}{\partial x_0} - u_{\mathrm{L1}}\frac{\partial u_{\mathrm{L1}}}{\partial x_0}\right)$$
$$-\beta_2(u_{\mathrm{G1}} - u_{\mathrm{L1}})\frac{\partial \alpha_1}{\partial t_0} + 3\gamma p_{\mathrm{G0}}\left[\alpha_1\frac{\partial R_1}{\partial x_0} - (3\gamma+1)R_1\frac{\partial R_1}{\partial x_0}\right],$$

$$K_4 = -(1-\alpha_0)\left(\frac{\partial p_{\mathrm{L1}}}{\partial x_1} + \frac{\partial u_{\mathrm{L1}}}{\partial t_1}\right) + \beta_1\alpha_0\frac{\partial}{\partial t_1}(u_{\mathrm{G1}} - u_{\mathrm{L1}}) + \alpha_0\frac{\partial \alpha_1 u_{\mathrm{L1}}}{\partial t_0} + \beta_1\alpha_0\left(u_{\mathrm{G1}}\frac{\partial u_{\mathrm{G1}}}{\partial x_0} - u_{\mathrm{L1}}\frac{\partial u_{\mathrm{L1}}}{\partial x_0}\right)$$
$$+\beta_1\alpha_0\alpha_1\frac{\partial}{\partial t_0}(u_{\mathrm{G1}} - u_{\mathrm{L1}}) + \beta_2\alpha_0(u_{\mathrm{G1}} - u_{\mathrm{L1}})\frac{\partial \alpha_1}{\partial t_0} + \alpha_0\alpha_1\frac{\partial p_{\mathrm{L1}}}{\partial x_0}$$
$$-(1-\alpha_0)\frac{\partial u_{\mathrm{L1}}^2}{\partial x_0} + \alpha_0\left[p_{\mathrm{L1}} + \left(\frac{\omega_{\mathrm{B}}^* R_0^*}{U^*}\right)^2 R_1\right]\frac{\partial \alpha_1}{\partial x_0},$$

$$K_5 = -\Omega^2\frac{\partial^2}{\partial t_0^2}R_1 - \frac{\Omega^2 V}{\Delta}\frac{\partial}{\partial t_0}\left(\frac{\Delta^2}{\Omega^2}R_1 + \sigma_1 d_0\right) + \frac{\Omega^2}{\Delta^2}\frac{3}{2}\gamma p_{\mathrm{G0}}(3\gamma+1)R_1^2 - \frac{\Omega^2}{\Delta^2}\sigma_2 R_1^2$$
$$-\frac{\Omega^2}{\Delta^2}\sigma_1(R_1 + d_0)^2 - \frac{\Omega^2}{\Delta^2}C_{\mathrm{ani}}\frac{\partial R_1}{\partial t_0} - \frac{\Omega^2}{\Delta^2}4\mu_{\mathrm{L}}\frac{\partial R_1}{\partial t_0} + \frac{\Omega^2}{\Delta^2}K_{\mathrm{ani}}R_1^2.$$

REFERENCES

[1] M. J. Blomley, J. C. Cooke, E. C. Unger, M. J. Monaghan, and D. O. Cosgrove, "Microbubble contrast agents: A new era in ultrasound," BMJ **322**, 1222–1225 (2001).

[2] A. Helbert, E. Gaud, T. Segers, C. Botteron, P. Frinking, and V. Jeannot, "Monodisperse versus polydisperse ultrasound contrast agents: In vivo sensitivity and safety in rat and pig," Ultrasound Med. Biol. **46**, 3339–3352 (2020).

[3] M. Versluis, E. Stride, G. Lajoinie, B. Dollet, and T. Segers, "Ultrasound contrast agent modeling: A review," Ultrasound Med. Biol. **46**, 2117–2144 (2020).

[4] T. Segers, L. De Rond, N. De Jong, M. Borden, and M. Versluis, "Stability of monodisperse phospholipid-coated microbubbles formed by flow-focusing at high production rates," Langmuir **32**, 3937–3944 (2016).

[5] M. A. Borden, P. Dayton, S. Zhao, and K. W. Ferrara, "Physico-chemical properties of the microbubble lipid shell [ultrasound contrast agents]," in *IEEE Ultrasonics Symposium* (IEEE, 2004), Vol. 1, pp. 20–23.

[6] B. Helfield, "A review of phospholipid encapsulated ultrasound contrast agent microbubble physics," Ultrasound Med. Biol. **45**, 282–300 (2019).

[7] A. J. Sojahrood, A. C. de Leon, R. Lee, M. Cooley, E. C. Abenojar, M. C. Kolios, and A. A. Exner, "Toward precisely controllable acoustic response of

shell-stabilized nanobubbles: High yield and narrow dispersity," ACS Nano **15**, 4901–4915 (2021).
[8]N. Teraphongphom, P. Chhour, J. R. Eisenbrey, P. C. Naha, W. R. Witschey, B. Opasanont, L. Jablonowski, D. P. Cormode, and M. A. Wheatley, "Nanoparticle loaded polymeric microbubbles as contrast agents for multimodal imaging," Langmuir **31**, 11858–11867 (2015).
[9]A. Upadhyay and S. V. Dalvi, "Synthesis, characterization and stability of BSA-encapsulated microbubbles," RSC Adv. **6**, 15016–15026 (2016).
[10]E. A. Maksimova, R. A. Barmin, P. G. Rudakovskaya, O. A. Sindeeva, E. S. Prikhozhdenko, A. M. Yashchenok, B. N. Khlebtsov, A. A. Solovev, G. Huang, Y. Mei *et al.*, "Air-filled microbubbles based on albumin functionalized with gold nanocages and zinc phthalocyanine for multimodal imaging," Micromachines **12**, 1161 (2021).
[11]N. de Jong, L. Hoff, T. Skotland, and N. Bom, "Absorption and scatter of encapsulated gas filled microspheres: Theoretical considerations and some measurements," Ultrasonics **30**, 95–103 (1992).
[12]C. C. Church, "The effects of an elastic solid surface layer on the radial pulsations of gas bubbles," J. Acoust. Soc. Am. **97**, 1510–1521 (1995).
[13]L. Hoff, P. C. Sontum, and J. M. Hovem, "Oscillations of polymeric microbubbles: Effect of the encapsulating shell," J. Acoust. Soc. Am. **107**, 2272–2280 (2000).
[14]P. Marmottant, S. Van Der Meer, M. Emmer, M. Versluis, N. De Jong, S. Hilgenfeldt, and D. Lohse, "A model for large amplitude oscillations of coated bubbles accounting for buckling and rupture," J. Acoust. Soc. Am. **118**, 3499–3505 (2005).
[15]K. Sarkar, W. T. Shi, D. Chatterjee, and F. Forsberg, "Characterization of ultrasound contrast microbubbles using *in vitro* experiments and viscous and viscoelastic interface models for encapsulation," J. Acoust. Soc. Am. **118**, 539–550 (2005).
[16]K. Tsiglifis and N. A. Pelekasis, "Nonlinear radial oscillations of encapsulated microbubbles subject to ultrasound: The effect of membrane constitutive law," J. Acoust. Soc. Am. **123**, 4059–4070 (2008).
[17]A. A. Doinikov, S. Zhao, and P. A. Dayton, "Modeling of the acoustic response from contrast agent microbubbles near a rigid wall," Ultrasonics **49**, 195–201 (2009).
[18]S. Paul, A. Katiyar, K. Sarkar, D. Chatterjee, W. T. Shi, and F. Forsberg, "Material characterization of the encapsulation of an ultrasound contrast microbubble and its subharmonic response: Strain-softening interfacial elasticity model," J. Acoust. Soc. Am. **127**, 3846–3857 (2010).
[19]G. Lajoinie, E. Linnartz, P. Kruizinga, N. De Jong, E. Stride, G. Van Soest, and M. Versluis, "Laser-driven resonance of dye-doped oil-coated microbubbles: A theoretical and numerical study," J. Acoust. Soc. Am. **141**, 2727–2745 (2017).
[20]Y. Liu, K. Sugiyama, and S. Takagi, "On the interaction of two encapsulated bubbles in an ultrasound field," J. Fluid Mech. **804**, 58–89 (2016).
[21]J. Sijl, B. Dollet, M. Overvelde, V. Garbin, T. Rozendal, N. De Jong, D. Lohse, and M. Versluis, "Subharmonic behavior of phospholipid-coated ultrasound contrast agent microbubbles," J. Acoust. Soc. Am. **128**, 3239–3252 (2010).
[22]A. A. Doinikov and P. A. Dayton, "Maxwell rheological model for lipid-shelled ultrasound microbubble contrast agents," J. Acoust. Soc. Am. **121**, 3331–3340 (2007).
[23]D. Chatterjee and K. Sarkar, "A Newtonian rheological model for the interface of microbubble contrast agents," Ultrasound Med. Biol. **29**, 1749–1757 (2003).
[24]D. A. Gubaidullin and Y. V. Fedorov, "Acoustics of a viscoelastic medium with encapsulated bubbles," J. Hydrodyn. **33**, 55–62 (2021).
[25]D. A. Gubaidullin, K. A. Panin, and Y. V. Fedorov, "Acoustics of a liquid with droplets covered by a shell in the presence of phase transitions," Fluid Dyn. **57**, 459–468 (2022).
[26]D. A. Gubaidullin, D. D. Gubaidullina, and Y. V. Fedorov, "Mathematical modeling of the wave dynamics of an encapsulated perfluorocarbon droplet in a viscoelastic liquid," Mathematics **11**, 1083 (2023).
[27]O. Couture, M. Fink, and M. Tanter, "Ultrasound contrast plane wave imaging," IEEE Trans. Ultrason., Ferroelectr., Freq. Control **59**, 2676–2683 (2012).
[28]K. W. Commander and A. Prosperetti, "Linear pressure waves in bubbly liquids: Comparison between theory and experiments," J. Acoust. Soc. Am. **85**, 732–746 (1989).
[29]A. J. Sojahrood, Q. Li, H. Haghi, R. Karshafian, T. M. Porter, and M. C. Kolios, "Pressure dependence of the ultrasound attenuation and speed in bubbly media: Theory and experiment," arXiv:1811.07788 (2018).
[30]A. J. Sojahrood, Q. Li, H. Haghi, R. Karshafian, T. M. Porter, and M. C. Kolios, "Investigation of the nonlinear propagation of ultrasound through a bubbly medium including multiple scattering and bubble-bubble interaction: Theory and experiment," in *2017 IEEE International Ultrasonics Symposium (IUS)* (IEEE, 2017), pp. 1–4.
[31]D. Fuster, J.-M. Conoir, and T. Colonius, "Effect of direct bubble-bubble interactions on linear-wave propagation in bubbly liquids," Phys. Rev. E **90**, 063010 (2014).
[32]A. J. Sojahrood, H. Haghi, R. Karshfian, and M. C. Kolios, "Probing the pressure dependence of sound speed and attenuation in bubbly media: Experimental observations, a theoretical model and numerical calculations," Ultrason. Sonochem. **95**, 106319 (2023).
[33]B. Helfield, X. Chen, B. Qin, and F. S. Villanueva, "Individual lipid encapsulated microbubble radial oscillations: Effects of fluid viscosity," J. Acoust. Soc. Am. **139**, 204–214 (2016).
[34]A. J. Sojahrood, R. Earl, H. Haghi, Q. Li, T. M. Porter, M. C. Kolios, and R. Karshafian, "Nonlinear dynamics of acoustic bubbles excited by their pressure-dependent subharmonic resonance frequency: Influence of the pressure amplitude, frequency, encapsulation and multiple bubble interactions on oversaturation and enhancement of the subharmonic signal," Nonlinear Dyn. **103**, 429–466 (2021).
[35]A. J. Sojahrood, H. Haghi, R. Karshafian, and M. C. Kolios, "Nonlinear dynamics and bifurcation structure of ultrasonically excited lipid coated microbubbles," Ultrason. Sonochem. **72**, 105405 (2021).
[36]A. J. Sojahrood, H. Haghi, T. M. Porter, R. Karshafian, and M. C. Kolios, "Experimental and numerical evidence of intensified non-linearity at the microscale: The lipid coated acoustic bubble," Phys. Fluids **33**, 072006 (2021).
[37]A. J. Sojahrood, H. Haghi, R. Karshafian, and M. C. Kolios, "Classification of the major nonlinear regimes of oscillations, oscillation properties, and mechanisms of wave energy dissipation in the nonlinear oscillations of coated and uncoated bubbles," Phys. Fluids **33**, 016105 (2021).
[38]K. E. Morgan, J. S. Allen, P. A. Dayton, J. E. Chomas, A. L. Klibaov, and K. W. Ferrara, "Experimental and theoretical evaluation of microbubble behavior: Effect of transmitted phase and bubble size," IEEE Trans. Ultrason., Ferroelectr., Freq. Control **47**, 1494–1509 (2000).
[39]J. Tu, J. Guan, Y. Qiu, and T. J. Matula, "Estimating the shell parameters of SonoVue® microbubbles using light scattering," J. Acoust. Soc. Am. **126**, 2954–2962 (2009).
[40]M. Overvelde, V. Garbin, J. Sijl, B. Dollet, N. De Jong, D. Lohse, and M. Versluis, "Nonlinear shell behavior of phospholipid-coated microbubbles," Ultrasound Med. Biol. **36**, 2080–2092 (2010).
[41]Y. Luan, T. Faez, E. Gelderblom, I. Skachkov, B. Geers, I. Lentacker, T. van der Steen, M. Versluis, and N. de Jong, "Acoustical properties of individual liposome-loaded microbubbles," Ultrasound Med. Biol. **38**, 2174–2185 (2012).
[42]B. L. Helfield and D. E. Goertz, "Nonlinear resonance behavior and linear shell estimates for Definity™ and MicroMarker™ assessed with acoustic microbubble spectroscopy," J. Acoust. Soc. Am. **133**, 1158–1168 (2013).
[43]I. Lentacker, I. De Cock, R. Deckers, S. C. De Smedt, and C. T. W. Moonen, "Understanding ultrasound induced sonoporation: Definitions and underlying mechanisms," Adv. Drug Delivery Rev. **72**, 49–64 (2014).
[44]T. Segers, N. De Jong, and M. Versluis, "Uniform scattering and attenuation of acoustically sorted ultrasound contrast agents: Modeling and experiments," J. Acoust. Soc. Am. **140**, 2506–2517 (2016).
[45]G. Chabouh, "Ultrasound contrast agents: From spherical oscillations and buckling dynamics to swimming," Ph.D. thesis (Université Grenoble Alpes, 2020).
[46]S. Spiekhout, J. Voorneveld, B. Van Elburg, G. Renaud, T. Segers, G. P. Lajoinie, M. Versluis, M. D. Verweij, N. De Jong, and J. G. Bosch, "Time-resolved absolute radius estimation of vibrating contrast microbubbles using an acoustical camera," J. Acoust. Soc. Am. **151**, 3993–4003 (2022).
[47]J. Birdi, S. V. Heymans, G. Collado-Lara, K. Van Den Abeele, J. D'hooge, and A. Bertrand, "Single-shot attenuation coefficient estimation for ultrasound contrast agents," Front. Phys. **10**, 1259 (2022).
[48]Q. N. Nguyen and T. Kanagawa, "Nonlinear ultrasound in liquid containing multiple coated microbubbles: Effect of buckling and rupture of viscoelastic shell on ultrasound propagation," Nonlinear Dyn. **111**, 10859–10877 (2023).
[49]A. Lytra and N. Pelekasis, "Static response of coated microbubbles compressed between rigid plates: Simulations and asymptotic analysis including elastic and adhesive forces," Phys. Fluids **30**, 030711 (2018).

[50]N. Pelekasis, M. Vlachomitrou, and A. Lytra, "Compression-only behavior: Effect of prestress and shell rheology on bifurcation diagrams and parametric stability of coated microbubbles in an unbounded flow," Phys. Rev. Fluids **7**, 113601 (2022).
[51]A. Lytra, V. Sboros, A. Giannakopoulos, and N. Pelekasis, "Modeling atomic force microscopy and shell mechanical properties estimation of coated microbubbles," Soft Matter **16**, 4661–4681 (2020).
[52]N. Dash and G. Tamadapu, "Describing the dynamics of a nonlinear viscoelastic shelled microbubble with an interface energy model," J. Appl. Phys. **132**, 204702 (2022).
[53]N. Dash and G. Tamadapu, "Radial dynamics of an encapsulated microbubble with interface energy," J. Fluid Mech. **932**, A26 (2022).
[54]D. Qin, Q. Zou, S. Lei, W. Wang, and Z. Li, "Cavitation dynamics and inertial cavitation threshold of lipid coated microbubbles in viscoelastic media with bubble–bubble interactions," Micromachines **12**, 1125 (2021).
[55]M. Vlachomitrou and N. Pelekasis, "Numerical study of the interaction between a pulsating coated microbubble and a rigid wall. I. Translational motion," Phys. Rev. Fluids **6**, 013601 (2021).
[56]M. Vlachomitrou and N. Pelekasis, "Numerical study of the interaction between a pulsating coated microbubble and a rigid wall. II. Trapped pulsation," Phys. Rev. Fluids **6**, 013602 (2021).
[57]D. Qin, S. Lei, X. Wang, X. Zhong, X. Ji, and Z. Li, "Resonance behaviors of encapsulated microbubbles oscillating nonlinearly with ultrasonic excitation," Ultrason. Sonochem. **94**, 106334 (2023).
[58]A. F. Abu-Bakr and A. K. Abu-Nab, "Growth of lipid-coated multi-microbubbles in viscoelastic tissues," Eur. Phys. J. Plus **137**, 513 (2022).
[59]J. Gümmer, S. Schenke, and F. Denner, "Modelling lipid-coated microbubbles in focused ultrasound applications at subresonance frequencies," Ultrasound Med. Biol. **47**, 2958–2979 (2021).
[60]D. Carugo, R. J. Browning, I. Iranmanesh, W. Messaoudi, P. Rademeyer, and E. Stride, "Scaleable production of microbubbles using an ultrasound-modulated microfluidic device," J. Acoust. Soc. Am. **150**, 1577–1589 (2021).
[61]I. O. Zalloum, A. A. Paknahad, M. C. Kolios, R. Karshafian, and S. S. Tsai, "Controlled shrinkage of microfluidically generated microbubbles by tuning lipid concentration," Langmuir **38**, 13021–13029 (2022).
[62]O. Louisnard, "A simple model of ultrasound propagation in a cavitating liquid. Part I: Theory, nonlinear attenuation and traveling wave generation," Ultrason. Sonochem. **19**, 56–65 (2012).
[63]A. J. Sojahrood, H. Haghi, R. Karshafian, and M. C. Kolios, "Nonlinear model of acoustical attenuation and speed of sound in a bubbly medium," in *2015 IEEE International Ultrasonics Symposium (IUS)* (IEEE, 2015), pp. 1–4.
[64]Y. Kikuchi and T. Kanagawa, "Weakly nonlinear theory on ultrasound propagation in liquids containing many microbubbles encapsulated by visco-elastic shell," Jpn. J. Appl. Phys. **60**, SDDD14 (2021).
[65]G. Chabouh, B. Dollet, C. Quilliet, and G. Coupier, "Spherical oscillations of encapsulated microbubbles: Effect of shell compressibility and anisotropy," J. Acoust. Soc. Am. **149**, 1240–1257 (2021).
[66]Y. Kikuchi, T. Kanagawa, and T. Ayukai, "Physico-mathematical model for multiple ultrasound-contrast-agent microbubbles encapsulated by a visco-elastic shell: Effect of shell compressibility on ultrasound attenuation," Chem. Eng. Sci. **269**, 117541 (2023).
[67]T. Kanagawa, M. Honda, and Y. Kikuchi, "Nonlinear acoustic theory on flowing liquid containing multiple microbubbles coated by a compressible visco-elastic shell: Low and high frequency cases," Phys. Fluids **35**, 023303 (2023).
[68]G. Chabouh, B. van Elburg, M. Versluis, T. Segers, C. Quilliet, and G. Coupier, "Buckling of lipidic ultrasound contrast agents under quasi-static load," Philos. Trans. R. Soc. A **381**, 20220025 (2023).
[69]J. Ma, J. Yu, Z. Fan, Z. Zhu, X. Gong, and G. Du, "Acoustic nonlinearity of liquid containing encapsulated microbubbles," J. Acoust. Soc. Am. **116**, 186–193 (2004).
[70]A. Prosperetti, "The thermal behaviour of oscillating gas bubbles," J. Fluid Mech. **222**, 587–616 (1991).
[71]M. Kameda and Y. Matsumoto, "Shock waves in a liquid containing small gas bubbles," Phys. Fluids **8**, 322–335 (1996).
[72]S. Kagami and T. Kanagawa, "Weakly nonlinear propagation of focused ultrasound in bubbly liquids with a thermal effect: Derivation of two cases of Khokolov–Zabolotskaya–Kuznetsoz equations," Ultrason. Sonochem. **88**, 105911 (2022).
[73]T. Kamei, T. Kanagawa, and T. Ayukai, "An exhaustive theoretical analysis of thermal effect inside bubbles for weakly nonlinear pressure waves in bubbly liquids," Phys. Fluids **33**, 053302 (2021).
[74]D. Fuster and F. Montel, "Mass transfer effects on linear wave propagation in diluted bubbly liquids," J. Fluid Mech. **779**, 598–621 (2015).
[75]L. Bergamasco and D. Fuster, "Oscillation regimes of gas/vapor bubbles," Int. J. Heat Mass Transfer **112**, 72–80 (2017).
[76]Y. Zhang, Y. Gao, Z. Guo, and X. Du, "Effects of mass transfer on damping mechanisms of vapor bubbles oscillating in liquids," Ultrason. Sonochem. **40**, 120–127 (2018).
[77]K. Yasui, J. Lee, T. Tuziuti, A. Towata, T. Kozuka, and Y. Iida, "Influence of the bubble-bubble interaction on destruction of encapsulated microbubbles under ultrasound," J. Acoust. Soc. Am. **126**, 973–982 (2009).
[78]H. Yusefi and B. Helfield, "The influence of inter-bubble spacing on the resonance response of ultrasound contrast agent microbubbles," Ultrason. Sonochem. **90**, 106191 (2022).
[79]T. Yatabe, T. Kanagawa, and T. Ayukai, "Theoretical elucidation of effect of drag force and translation of bubble on weakly nonlinear pressure waves in bubbly flows," Phys. Fluids **33**, 033315 (2021).
[80]S. Arai, T. Kanagawa, and T. Ayukai, "Nonlinear pressure waves in bubbly flows with drag force: Theoretical and numerical comparison of acoustic and thermal and drag force dissipations," J. Phys. Soc. Jpn. **91**, 043401 (2022).
[81]R. Egashira, T. Yano, and S. Fujikawa, "Linear wave propagation of fast and slow modes in mixtures of liquid and gas bubbles," Fluid Dyn. Res. **34**, 317–334 (2004).
[82]T. Yano, T. Kanagawa, M. Watanabe, and S. Fujikawa, "Nonlinear wave propagation in bubbly liquids," in *Bubble Dynamics and Shock Waves* (Springer, 2013), pp. 107–140.
[83]A. Jeffrey and T. Kawahara, *Asymptotic Methods in Nonlinear Wave Theory* (Pitman, London, 1982).
[84]T. Kanagawa, T. Yano, M. Watanabe, and S. Fujikawa, "Unified theory based on parameter scaling for derivation of nonlinear wave equations in bubbly liquids," J. Fluid Sci. Technol. **5**, 351–369 (2010).
[85]M. Guédra, C. Cornu, and C. Inserra, "A derivation of the stable cavitation threshold accounting for bubble-bubble interactions," Ultrason. Sonochem. **38**, 168–173 (2017).
[86]N. de Jong, P. J. Frinking, A. Bouakaz, and F. J. Ten Cate, "Detection procedures of ultrasound contrast agents," Ultrasonics **38**, 87–92 (2000).
[87]F. Forsberg, W. T. Shi, and B. B. Goldberg, "Subharmonic imaging of contrast agents," Ultrasonics **38**, 93–98 (2000).